AIAA JOURNAL
Vol. 33, No. 12, December 1995

Hierarchical Bending Analysis of Cord-Rubber Composites

R. M. V. Pidaparti*
Purdue University at Indianapolis, Indianapolis, Indiana 46202

The bending stiffness of twisted steel cords and two-ply steel reinforced rubber belt structure was investigated using a hierarchical three-dimensional beam finite element analysis. The three-dimensional beam element takes into account the coupled extension, bending, and twisting deformations. The finite element results of bending stiffness obtained for twisted cords and two-ply cord-rubber belt are compared to the experimental data and other alternate solutions available in the literature. The effects of cord orientation, anisotropy, twisted nature of cords, and rubber core surrounding the twisted cord on the bending stiffness properties are presented and discussed.

Nomenclature

A	= nondimensional area, A_c/R^2
A_c	= cross-sectional area of cord
b	= specimen width
c, c_1, c_2, c_3, c_4	= cord constants to define extension-twisting coupling
D_x	= bending stiffness of the laminate in four-point bending
d	= yarn/filament diameter in the cord
d^*	= center distance between yarn/filament and cord
$\bar{E}$	= nondimensional modulus, E_m/E_c
E_c	= modulus of elasticity of cord material
E_c^i	= modulus of elasticity of ith filament in the cord material
E_m	= modulus of elasticity of matrix (rubber) material
E_1, E_2	= unidirectional lamina modulus of elasticity
G_c	= shear modulus of cord material
G_m	= shear modulus of matrix (rubber) material
G_{12}	= unidirectional lamina shear modulus
h	= total laminate thickness
$\bar{h}$	= nondimensional thickness, h/R
L	= length of the laminate
P	= applied load
R	= radius of the cord
R_i	= center filament/yarn radius
tpi_{yarn}	= number of twists/unit length for yarn
tpi_{cord}	= number of twists/unit length for cord
v_c	= volume fraction of cords
v_m	= volume fraction of matrix (rubber) material
α, β	= twist angle for yarn and cord, respectively
δ	= deflection under the load in four-point bending experiment
ν_c	= Poisson's ratio of the cord material
ν_m	= Poisson's ratio of the matrix material
ν_{12}	= major Poisson's ratio of unidirectional lamina

Introduction

CORD-RUBBER composite laminates find applications in aerospace and automotive engineering industries, especially for tires, airsprings, conveyer belts, sonar domes in military applications, etc. Cord-rubber composites have several unique features compared to rigid matrix composites. Some of the features include a degree of anisotropy of the order of 10,000, large deformation of the rubber material, and the twisted nature of the cords, among others. It is quite difficult to characterize a cord as well as a cord-rubber ply. Experimental determination of twisted cord stiffness properties is extremely difficult. Cord itself is not a single filament but many filaments twisted together. When a cord-rubber laminate is subjected to tension, it also bends and twists. Because of the complexity of cord construction, these composites exhibit coupled extension-bending-twisting behavior when subjected to loading. It is important to capture the bending-twisting and extension-twisting behavior for realistic analysis of cord-rubber laminates.

Analytical studies have been carried out to investigate the response of two-ply cord-rubber laminates subjected to different loading conditions.[1–5] Hirano and Akasaka[1] and Akasaka et al.[2] analytically studied the coupled extension-torsion and bending-shear deformations of cord-rubber laminates subjected to extension and bending loadings. They developed explicit equations for stiffness by taking into account the interlaminar shear deformation. Robbins and Clark[3] presented an engineering analysis of bending stiffness of cord-rubber laminates based on laminate theory. They did not consider the interlaminar shear or coupled bending shear deformations. Bert[4] presented a theoretical treatment to predict the out-of-plane bending stiffness of a laminated composite plate under cylindrical bending based on classical lamination theory. The bending behavior of steel cord-rubber laminates was studied by Akasaka et al.[5] by including the interply shear deformation and bending-shear deformations. Recently, Shield and Costello[6] studied the bending of single-ply and two-ply cord-rubber composite plates using an equilibrium approach based on Kirchhoff plate theory by including the extension-twisting coupling behavior.

There are a number of two- and three-dimensional finite element studies of cord-rubber composites, Refs. 7–9, among others. Turner and Ford[8] showed experimentally that significant interply shear strains exist when a two-ply composite is subjected to simple tension. These interply shear strains are believed to be mainly responsible for fatigue induced delamination. Ford et al.[9] applied the axisymmetric finite element method to the Turner and Ford model. Hsieh[10] and Cembrola and Dudek[11] presented finite element models to study the behavior of cord-rubber laminates. De Eskinazi et al.[12] compared the results of interply shear strains from two- and three-dimensional finite element analysis and showed that the results were much different when three-dimensional analysis was used. Recently, Pidaparti and Kakarla[13] presented a three-dimensional finite element model to study the extensional behavior of two-ply cord-rubber composite laminates. The results indicated that coupled bending-shear and twisting-shear deformations are important for a realistic analysis of the behavior of two-ply cord-rubber composites. There were no studies dealing with bending analysis of cord-rubber composites that take into account the coupled axial, bending, and twist deformations.

In this study, the bending of cord-rubber composite laminates was investigated using a hierarchical three-dimensional beam finite element model. The present model takes into account the extension-bending-twisting couplings due to cord construction. The finite element results of bending stiffness obtained for a two-ply cord rubber-composite laminate under four-point bending loading are compared to the existing experimental data and analytical models of simple bending theory and cylindrical bending theory. The effects

Received Oct. 31, 1994; revision received Feb. 7, 1995; accepted for publication Feb. 20, 1995.

*Associate Professor, Department of Mechanical Engineering, 723 W. Michigan Street. Senior Member AIAA.

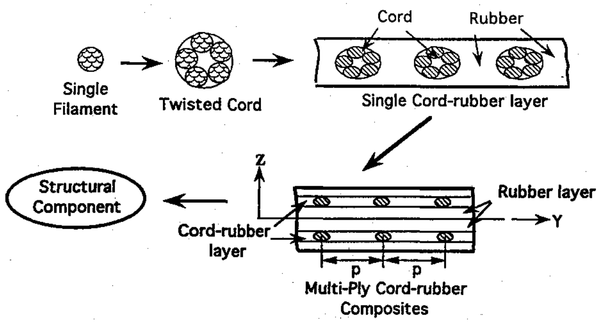

Fig. 1 Hierarchy in cord-rubber composites.

of cord orientation, anisotropy, twisted nature of cords, and rubber core surrounding the twisted cord on the bending stiffness properties were presented. These predicted bending stiffness and the hierarchical finite element model presented would help in better understanding the mechanical behavior of cord-rubber composite materials.

Hierarchical Finite Element Analysis

Figure 1 shows a hierarchy of cord-rubber laminates. Three different levels of hierarchy have been identified for cord-rubber composites. At the ultrastructural level there is a single twisted filament, at the microstructural level a twisted cord consists of a number of filaments twisted together, and at the macrostructural level a number of twisted cords are put into a rubber material to form a unidirectional cord-reinforced rubber sheet. These reinforced rubber sheets are utilized with different cord-orientation and rubber thicknesses to form a structural component such as a belt or tire. Hierarchy in terms of different microstructures exists in natural composites like wood and bone. We can use the hierarchy to model different structures using finite element analysis to achieve efficient design of composite structures. Recently, Sreenivasan and Cassenti[14] demonstrated through a preliminary study that composite structures can be designed from a hierarchical approach to achieve tough composites with some reduction in stiffness.

In the present study, a recently developed three-dimensional beam finite element model for twisted cords by Pidaparti[15] was used to investigate the bending analysis of twisted cords and cord-rubber laminates by modifying the computer program. Two levels of finite element modeling were done, first for a twisted cord in three-point bending and then for the two-ply cord-rubber laminate under four-point bending. Both the twisted cord and the cord-rubber laminate are modeled as beam structures. The present beam element is a three-node isoparametric finite element. The cross section of the beam is modeled using eight-node isoparametric finite elements. The present finite element model takes into account stiffness couplings due to axial, bending, twisting, and warping deformations. The finite element has beam nodes and warping nodes. Each beam node has three translational degrees of freedom (DOF) and three rotational degrees of freedom, respectively. Each warping node has a single DOF in the beam direction but normal to the deformed cross section. The details of this beam element can be found in Ref. 15. Linear elastic analysis is carried out with different material models described subsequently. The bending stiffness of two-ply composite as well as the twisted cord are obtained from the finite element analysis to illustrate the hierarchical approach to cord-rubber composite structures.

Material Models for Cord-Rubber Composite Lamina

Two material models were used in the present study for a single ply cord-rubber composite lamina, the details of which are described as follows.

Material Model 1

This material model treats a cord-rubber ply as an orthotropic material and was developed for cord-rubber composites by Akasaka and Hirano.[16] This material model assumes that there is a large difference in moduli between cord and rubber and does not take into account the twisted nature of the cords. This material model is defined by four constants. The Akasaka–Hirano equations are given by

$$\begin{aligned} E_1 &= E_c v_c \\ E_2 &= 4E_m/3 \\ G_{12} &= G_m \\ \nu_{12} &= 0.5 \end{aligned} \tag{1}$$

Material Model 2

This material model assumes that the unidirectional lamina is monocyclic and takes into account the twisted nature of cords. It was developed by Shield and Costello.[17] This material model was derived from an energy approach and the Shield–Costello equations are given by

$$E_1 = E_m + c_1 E_c v_c \left[1 - \frac{6c_2 c_3 v_c (1+\nu_m)}{c_1 \left(\bar{A}\bar{h}^2 \bar{E} + 6 c_4 v_c (1+\nu_m)\right)} \right] \tag{2}$$

$$E_2 = \frac{4E_m[c_1 E_c v_c + E_m] + \left\{[24(1+\nu_m)v_c E_c]/\bar{A}\bar{h}^2\right\}(c_4 E_m + C E_c v_c)}{\left[4E_m + 4\left(1-\nu_m^2\right)v_c c_1 E_c + \left\{[24(1+\nu_m)v_c]/\bar{A}\bar{h}^2 \bar{E}\right\}\left(c_4 E_m + C E_c v_c\left(1-\nu_m^2\right)\right)\right.} \tag{3}$$

$$\begin{aligned} G_{12} &= G_m(1 - v_c) \\ \nu_{12} &= \nu_m \end{aligned} \tag{4}$$

where ν_m is Poisson's ratio of rubber material, and $\bar{A} = A_c/R^2$, $\bar{h} = h/R$, and $\bar{E} = E_m/E_c$. A_c is the area of the cord, h is the thickness of cord-rubber ply, R is the outer radius of the cord, and v_c is the cord volume fraction. The constants c_1, c_2, c_3, c_4 and $c = c_1c_4 - c_2c_3$ are used to describe the extension-twisting coupling which are determined analytically by Shield and Costello.[17] These constants depend on the helix angle of the cord and the ratio of inner wire diameter to outer wire diameter. Recently, Shield and Costello[17] applied this material model to study the mechanical behavior of single ply and two-ply cord rubber composite plates. Material models 1 and 2 were included in the present finite element model.

Material Model for Twisted Cords

A typical cord in cord-rubber composites consists of a number of filaments/yarns twisted together. Each filament (diameter d) can have a different number of twists per unit length of the cord. The material properties for the cord can be described by Young's modulus E_c and Poisson's ratio ν_c. The cord stiffness properties vary according to number of twists/unit length and the relative packing between the filaments. Young's modulus for a twisted cord is assumed[18] as

$$E_c^i = E_f \cos^4\beta \cos^2\alpha \left[1 - 1.5\tan^2\beta \left(1 + \frac{2\log\cos\alpha}{\sin^2\alpha} \right) \right] \tag{5}$$

where E_c^i is a contribution by a typical ith filament, and the total cord modulus E_c is obtained by summing over the number of filaments in the cord. In Eq. (5) α and β are defined as

$$\begin{aligned} \tan\alpha &= \Pi d tpi_{\text{yarn}} \\ \tan\beta &= \Pi d^* tpi_{\text{cord}} \end{aligned} \tag{6}$$

where d is the diameter of the filament or yarn, d^* is the distance between the filament centerline and the cord axis, and tpi_{yarn} and

tpi_{cord} are the number of twists per unit length of the cord. The expression for Young's modulus of twisted cords was compared to the controlled experimental data with good agreement.[18] A value of Poisson's ratio is assumed for the cords. Sometimes, it can be obtained from single-ply properties by backward calculations using one of the theories for single-ply composites.[16] The shear modulus for the cord is calculated using the relationship for an isotropic material as

$$G_c = E_c/2(1+\nu_c) \tag{7}$$

The Eq. (5) material model for twisted cords was also included in the present finite element model to estimate the stiffness of individual cord as combination of rubber and cords.

Results and Discussion

Two levels of finite element analysis were carried out to estimate 1) the bending stiffness of a two-ply steel cord rubber composite strip having $\pm\alpha$ cord orientation under four-point bending loading and 2) the bending stiffness of a twisted steel cord under three-point bending loading. The geometry of the steel cord-rubber specimen subjected to four-point bending loading is shown in Fig. 2. This geometry is considered for the stress analysis because the experimental data and alternate solutions are available in the literature for comparison. The length of the specimen $L = 200$ mm, width $b = 80$ mm, and thickness $H = 1.8$ mm. The distance between the loading points is $a = 80$ mm. Figure 3a shows the cross section details of the cord-rubber specimen. The cord-rubber layer has a thickness of $h = 0.676$ mm, the two rubber layers have thicknesses of 0.65 mm, and the outer rubber layers have a thickness of 0.312 mm. Figure 3b shows the cross section details of the twisted cord of the specimen. Four different cord orientations, from 15 to 30 deg for which the experimental data is available, are considered in this study. The following material properties were used for the finite element analysis and were obtained from Ref. 5.

Rubber properties:

$$E_m = 5.0 \text{ MPa} \qquad \nu_m = 0.49$$

A thickness of 0.1 mm of rubber material surrounding the cord was used.

Steel cord geometric and material properties:

$$E_c = 210.0 \text{ GPa} \qquad \nu_c = 0.3$$

$$\text{number of yarns} = 5 \qquad tpi_{yarn} = 5$$

$$d = 0.25 \text{ mm} \qquad tpi_{cord} = 3$$

$$d^* = 0.213 \text{ mm} \qquad \text{helix angle} = 81.4 \text{ deg}$$

$$R_i = 0.088 \text{ mm} \qquad \nu_c = 0.2976$$

$$c_1 = 0.967 \qquad c_2 = 0.0828$$

$$c_3 = 0.187 \qquad c_4 = 0.0723$$

The constants for twisted cords were taken from Ref. 17.

Steel cord-rubber composite properties:

$$E_1 = 62.5 \text{ GPa} \qquad E_2 = 9.49 \text{ MPa}$$

$$G_{12} = 2.39 \text{ MPa} \qquad \nu_{12} = 0.43$$

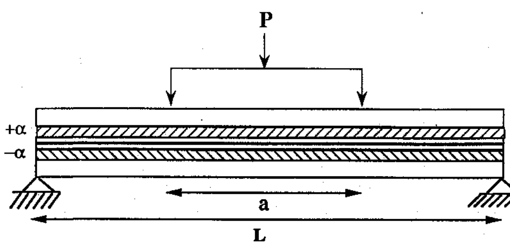

Fig. 2 Four-point bending of a two-ply steel cord-rubber composite specimen.

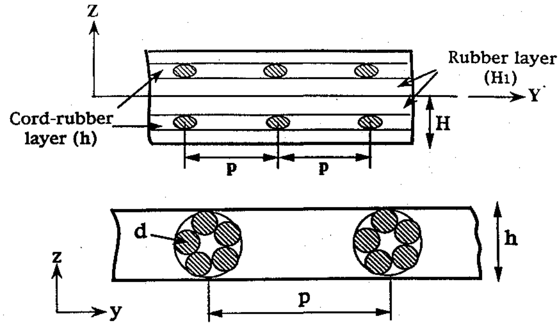

Fig. 3 Cross-section details of the two-ply steel cord-rubber composite specimen.

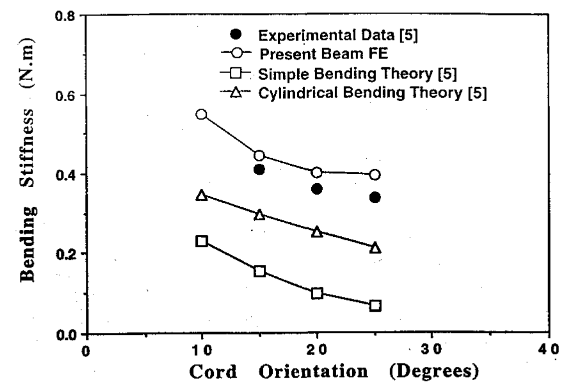

Fig. 4 Comparison of bending stiffness variation with cord orientation for the two-ply steel cord reinforced rubber composite laminate.

where the subscripts 1 and 2 refer to the directions parallel to the cord and transverse to the cord, respectively.

Validation

A two-ply cord-rubber composite strip was modeled as a five-ply system with two layers of cord-rubber material surrounded by three layers of rubber material. This representation led to better results since the cord contribution is smeared out over a layer of the thickness of cords. A converged finite element mesh of $4 \times 4 \times 6$ (length $\times$ width $\times$ thickness) was used to model the two-ply composite using the present finite element model. The results of bending stiffness obtained by the present finite element model are validated by comparing with the analytical and experimental data.[5] The bending stiffness is calculated using the formula

$$D_x = a^2 P(L-a)/32b\delta \tag{8}$$

where δ is the deflection at the midpoint under the applied load. Figure 4 shows the comparison of bending stiffness for cord orientations of 10–30 deg for the two-ply cord-rubber composite specimen considered. It can be seen that good agreement is found between the present finite element results and the experimental data.[5] The simple bending theory and the cylindrical bending theory[5] underestimated the bending stiffness as compared to the experimental data. The bending stiffness decreases as the cord orientation is increased. Good agreement of the results validates the utility of the present finite element model for two-ply cord rubber composites subjected to bending loading.

Effect of Anisotropy

Figure 5 shows the effect of anisotropy (ratio of cord modulus to rubber modulus) on the bending stiffness for a cord orientation of 20 deg for the two-ply cord-rubber composite specimen shown in Fig. 3. In other words, the results presented in Fig. 5 indicate that the bending stiffness of the laminate increases as the cord modulus is increased while keeping the rubber modulus constant. It can be seen from Fig. 5 that the two-ply composite bending stiffness increases nonlinearly with increasing cord/rubber modulus.

Table 1 Comparison of bending rigidity of steel cords

Reference	Bending rigidity, N · m
Approximate value[5]	0.165
Present FE (material model 1)	0.105
Present FE (material model 2)	0.116
Experiment[5]	0.121

Table 2 Comparison of bending stiffness of twisted steel cords with and without surrounding rubber material under three-point bending

Present finite element	Bending stiffness without rubber, N · m	Bending stiffness with rubber, N · m
Material model 1	0.721	0.823
Material model 2	0.673	0.785

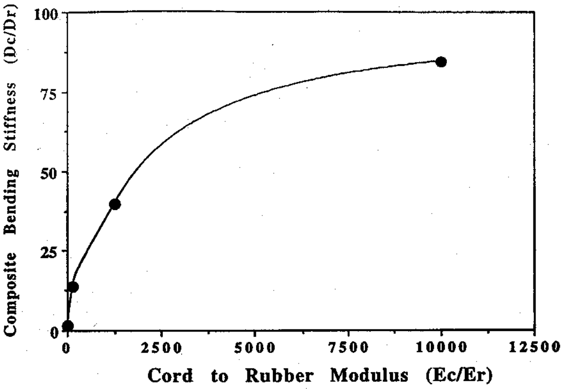

Fig. 5 Variation of bending stiffness with cord to rubber modulus for a 20-deg two-ply steel cord reinforced rubber composite laminate.

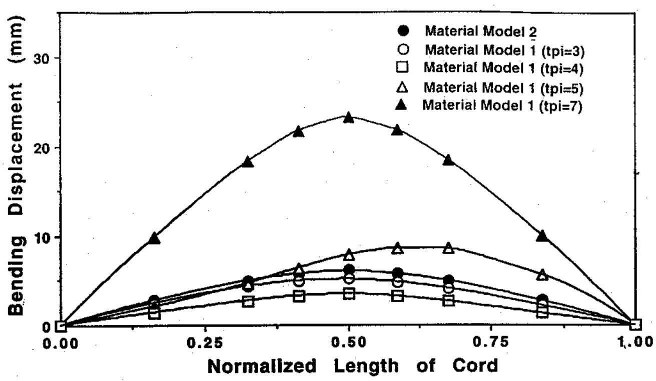

Fig. 6 Variation of bending displacement along the length of the cord for a twisted steel cord using the two material models.

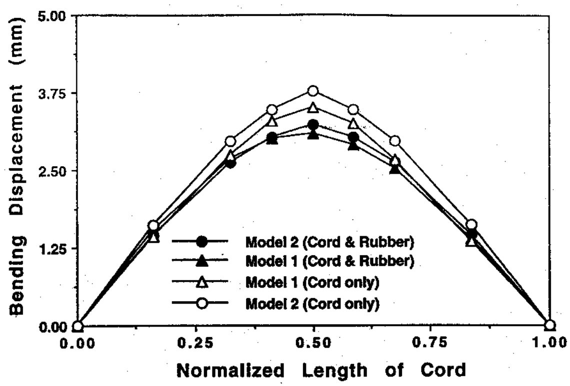

Fig. 7 Variation of bending displacement along the length of the twisted steel cord with and without surrounding rubber material.

The bending stiffness increases by about 85% when the cord modulus is increased by 10,000 times that of rubber modulus.

Cord Bending Stiffness

The cross section of a unidirectional cord reinforced rubber layer, in which each cord is arranged with a constant pitch p as considered by Akasaka et al.,[5] is shown in Fig. 3. The thickness of cord is $h = 0.676$ mm and consists of five thin filaments of diameter $d = 0.25$ mm. Akasaka et al.[5] evaluated the bending stiffness by conducting a three-point bending test for a twisted cord. They also used an approximate value for the bending stiffness of cord by summing the rigidities of five constituent filaments. They did not consider the fact that these constituent filaments are twisted together along a core cylinder of rubber filler into a single cord. In the present study, we considered the effect of the twisted nature of the cord as well as the rubber core surrounding the cord. Table 1 shows the comparison of bending stiffness (stiffness/unit thickness) of cord with experimental data of Akasaka et al.[5] Model 1 predicts lower bending stiffness as compared to model 2. It can be seen that good agreement is found between the experimental data and the present model 2 when the twisted nature of the cords is included in the finite element (FE) model.

Effect of Rubber Core Surrounding the Cord

Figure 6 shows the results of bending displacement along the length of the cord using the present two material models. Both the models gave approximately the same results when the $tpi_c = 4$ was used in model 1. Also, model 2 results in symmetrical displacement about the loading line, whereas material model 1 gives skewed results for the bending displacement for different twists per unit length of the cord. As the number of tpi_c are increased, the bending displacement also increases. The increase is rapid when the tpi_c are higher.

Figure 7 shows the effect of rubber core of the twisted cord on the bending displacement for the present two material models considered. It can be seen from Fig. 7 that model 1 bending displacements are lower than model 2 displacements. When the rubber core is added to the twisted cord, both models gave approximately the same results. The effect of the rubber core around the twisted cord is to decrease the bending displacement by about 14 and 20% for models 1 and 2, respectively. Table 2 shows the effect of rubber core on the bending stiffness for the twisted cord. It can be seen from Table 2 that there is about a 15% increase in bending stiffness when a rubber core of 0.1 mm is used around the twisted cords. These results illustrate the practicability of the present finite element model for twisted cords as well as for two-ply cord-rubber composites.

Conclusions

The bending stiffness of twisted steel cords and two-ply steel reinforced rubber belt structure were investigated using a hierarchical finite element analysis. A three-dimensional beam element which takes into account the coupled extension, bending, and twisting deformations was used to investigate the bending stiffness. The finite element results of bending stiffness obtained for twisted cords and a two-ply cord-rubber belt are compared with the experimental data available in the literature and show good agreement. The effect of anisotropy of cord-rubber moduli is to increase the bending stiffness very rapidly in a nonlinear fashion. Both the twists/unit length and rubber core surrounding the cord increase the bending stiffness. The finite element model developed and the results of bending stiffness presented illustrate the utility of the hierarchical approach for cord-rubber composites.

Acknowledgment

This work is supported by the U.S. National Science Foundation through Grant MSS-9109683.

References

[1]Hirano, M., and Akasaka, T., "Coupled Deformation of an Asymmetrically Laminated Plate," *Journal of Composite Materials and Structures*, Vol. 2, 1973, pp. 6–11.

[2]Akasaka, T., Hirano, M., and Motomura, K., "In-plane Bending Rigidity of Biasply Laminated Composite Strip," *Journal of Composite Materials and Structures*, Vol. 3, 1974, pp. 12–16.

[3]Robbins, D. H., and Clark, S. K., "Bending Characteristics of Textile-cord Reinforced Rubber," American Society of Mechanical Engineers, ASME 64-WA/RP-7, 1964, pp. 1–12.

[4]Bert, C. W., "Simplified Prediction of Ply Steer in Radial Tires," *Journal of Tire Science and Technology*, Vol. 8, 1980, pp. 3–9.

[5]Akasaka, T., Kabe, K., and Sako, K., "Bending Stiffness of a Tire-belt Structure with Steel Cords," *Composites Science and Technology*, Vol. 24, 1985, pp. 215–230.

[6]Shield, C. K., and Costello, G. A., "Bending of Cord Composite Plates," *Journal of Engineering Mechanics*, Vol. 120, No. 4, 1994, pp. 876–892.

[7]Patel, H. P., Turner, J. L., and Walter, J. D., "Radial Tire Cord-Rubber Composites," *Rubber Chemistry and Technology*, Vol. 49, 1976, pp. 1095–1110.

[8]Turner, J. L., and Ford, J. L., "Interply Behavior Exhibited in Complimentary Composite Laminates," *Rubber Chemistry and Technology*, Vol. 55, 1982, pp. 1079–1094.

[9]Ford, J. L., Patel, H. P., and Turner, J. L., "Interlaminar Shear Effects in Cord-Rubber Composites," *Composite Science and Technology*, Vol. 17, 1982, pp. 255–271.

[10]Hsieh, K. T., "Modeling of Cord-Reinforced Rubber Laminates," Ph.D. Thesis, Univ. of Texas, Austin, TX, 1985.

[11]Cembrola, R. J., and Dudek, T. J., "Cord/rubber Material Properties," *Rubber Chemistry and Technology*, Vol. 58, No. 4, 1985, pp. 830–856.

[12]De Eskinazi, J., Ishihara, K., Volk, H., and Warholic, T. C., "Towards Predicting Relative Belt Edge Endurance with the Finite Element Method," *Journal of Tire Science and Technology*, Vol. 18, No. 4, 1990, pp. 216–235.

[13]Pidaparti, R. M. V., and Kakarla, V. P., "Three-Dimensional Stress Analysis of Two-Ply Cord-Rubber Composite Laminates," *Journal of Composite Structures*, Vol. 28, 1994, pp. 433–440.

[14]Sreenivasan, A. V., and Cassenti, B. N., "Hierarchy in the Design and Development of Structural Components: A Preliminary Study," *AIAA Journal*, Vol. 32, No. 9, 1994, pp. 1933–1935.

[15]Pidaparti, R. M. V., "Stiffness Characteristics of Twisted Cords for Cord-rubber Composites," *Journal of Composite Structures*, Vol. 24, 1993, pp. 291–298.

[16]Akasaka, T., and Hirano, M., "Approximate Elastic Constants of Fiber Reinforced Rubber Sheet and its Composite Laminate," *Composite Materials and Structures*, Vol. 1, 1972, pp. 70–76.

[17]Shield, C. K., and Costello, G. A., "The Effect of Wire Rope Mechanics on the Mechanical Response of Cord Composite Laminates: An Energy Approach," *Journal of Applied Mechanics*, Vol. 61, No. 3, 1994, pp. 9–15.

[18]Moghe, S. R., "Design of Fabric Reinforced Composites," *Textile Structural Composites*, Vol. 3, edited by T. S. Chou and F. K. Ko, Elsevier, New York, 1990, pp. 355–377.